

43rd Annual Symposium of the Ultrasonic Industry Association, UIA Symposium 2014

Multi-modal ultrasound imaging for breast cancer detection

L. Medina-Valdés^a, M. Pérez-Liva^b, J. Camacho^a, J.M. Udías^b, J.L. Herraiz^c, N. González-Salido^a

^a ITEFI, Spanish National Research Council (CSIC), Madrid, Spain.

^b Grupo de Física Nuclear, Dpto. Física Atómica, Molecular Nuclear, Universidad Complutense, CEI Moncloa, Madrid, Spain.

^c Madrid-MIT M+VISION Consortium, Massachusetts Institute of Technology (MIT), Boston, USA.

Abstract

This work describes preliminary results of a two-modality imaging system aimed at the early detection of breast cancer. The first technique is based on compounding conventional echographic images taken at regular angular intervals around the imaged breast. The other modality obtains tomographic images of propagation velocity using the same circular geometry. For this study, a low-cost prototype has been built. It is based on a pair of opposed 128-element, 3.2 MHz array transducers that are mechanically moved around tissue mimicking phantoms. Compounded images around 360° provide improved resolution, clutter reduction, artifact suppression and reinforce the visualization of internal structures. However, refraction at the skin interface must be corrected for an accurate image compounding process. This is achieved by estimation of the interface geometry followed by computing the internal ray paths. On the other hand, sound velocity tomographic images from time of flight projections have been also obtained. Two reconstruction methods, Filtered Back Projection (FBP) and 2D Ordered Subset Expectation Maximization (2D OSEM), were used as a first attempt towards tomographic reconstruction. These methods yield useable images in short computational times that can be considered as initial estimates in subsequent more complex methods of ultrasound image reconstruction. These images may be effective to differentiate malignant and benign masses and are very promising for breast cancer screening.

PACS: 43.35 Wa; 43.35.Bf

© 2015 The Authors. Published by Elsevier B.V. This is an open access article under the CC BY-NC-ND license

(<http://creativecommons.org/licenses/by-nc-nd/4.0/>).

Peer-review under responsibility of the Ultrasonic Industry Association

Keywords: image compounding, ultrasound tomography, breast cancer screening, CT, PET

1. Introduction

Breast Cancer is the malignant tumor with highest incidence in women and one of highest mortality rates, with 8 million new cases in the world each year (Jemal et al., 2011). However, survival rates are nearly 100% if detected at early stages (Breast cancer, 2014). In this context, mammogram screening programs were developed. However, mammography presents radiation risk and moderate sensitivity, especially in dense breast tissue, which is more likely to develop cancer (Ursin et al., 2005). Promising alternatives are the tomographic ultrasound imaging systems.

The potential of ultrasound computer tomography (USCT) potentials has been known since the 1970s (Schomberg, 1978). Those systems generate different image modalities, providing a performance comparable to Magnetic Resonance Imaging (Ranger et al., 2012), considered the gold standard. Furthermore, scanning is completely automated, so repetitive images are produced, allowing patient follow-up. USCT provides a full perspective of the mamma, so potential lesions can be located accurately. Ultrasound tomography also minimizes some drawbacks of conventional echography. As all insonification angles can be covered, biological structures are fully depicted, image noise due to speckle is reduced and spatial resolution is isotropic. However, the huge data volume involved and the time required to reconstruct images make ultrasound tomography unaffordable for clinical applications. Recently, first models have become available, even though, they still require high performance processing (Roy et al., 2013; Wiskin et al., 2010).

The USCT prototype developed in ARTEMIS project claims to offer automated and multi-modal ultrasonic imaging at reasonable cost. On one hand, Full Angle Spatial Compounding (FASC) is provided during scanning process in real time. This reflectivity image is the outcome of the average of conventional sector echographic images acquired 360° around the breast. FASC imaging reduces speckle and improves contrast to noise ratio. At the same time, angle-dependent artifacts are avoided, so biological structures are fully depicted.

On the other hand, ultrasound computer tomography may offer post-processing high quality reflectivity speed-of-sound images. In this work, we present a straight ray approximation to reconstruct real data from our experimental system. These kinds of approximations are very common in geometrical acoustics to easily obtain images with restriction of the maximum achievable resolution of $\lambda/2$. Two commonly used ray-tracing methods for CT and PET reconstruction (FBP and 2D OSEM) were implemented in order to obtain first attempt tomographic images, which not only give general information about structures under study but also can be usable as input to guide convergence of full wave algorithms.

The USCT system is based on conventional medical grade probes, arranged around the region of interest, configuring a ring aperture. Several 2D slices can be acquired by shifting the ring array along the coronal axis, which allows a complete 3D reconstruction of the breast, from nipple to armpit.

2. Materials and Methods

2.1. The USCT prototype

The experimental arrangement consists of 2 coplanar medical, 128-element, linear array transducers, of 3.2 MHz and 50% of bandwidth (Prosonic, Korea). These can be independently and accurately positioned around a breast phantom by means of a stepper motor with high mechanical resolution (0.1°). The array probes and the breast phantom are arranged inside a water tank to have good ultrasound coupling. The stepper motors are individually controlled by our own designed drivers with a USB interface. Beam steering and dynamic depth focusing are performed by ultrasonic equipment, SITAU 112 (Dasel, Spain). Data are transferred through another USB interface to a computer that performs post-processing and motor control in MATLAB (The Mathworks, USA).

FASC requires that the intersection of all sector images include the whole breast. Moreover, ACT algorithms require insonification of all imaged points for all transmitter positions in the ring aperture. To this purpose, the medical grade array probes have good lateral sensitivity (-6dB @ 45°).

A calibration process is performed prior to data acquisition to deal with mechanical inaccuracies in turning radius (R), angular deviation of the array transducers (β) and actual speed of sound in the coupling medium (water). As a result, array elements are accurately positioned in a global coordinate system.

2.2. Full Angle Spatial Compounding

Full Angle Spatial Compounding (FASC) is the reflectivity image from the average of sector images acquired from several angular positions around the breast. B-Mode images are acquired at regular angles around the region of interest (ROI) of 60 mm of radius, where all images overlap, with one probe in phased-array mode.

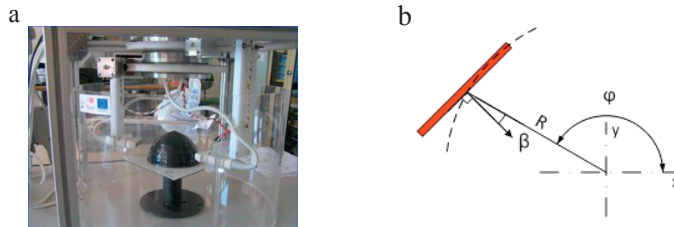


Fig. 1. (a) Experimental arrangement; (b) Reference coordinates and nomenclature

The sampling frequency is 20 MHz, the depth range is within 5 to 180 mm, and the lines are spaced 0.46° in the interval -55° to 55° . B-Mode images are scan converted and averaged on a rectangular pixel matrix. Pixel resolution is 0.15 mm for an estimated spatial resolution of 0.6 mm, which meets the Nyquist criterion in terms of spatial frequency.

In conventional echography, homogeneous speed of sound is assumed. However, the different breast tissues compose a heterogeneous medium. This leads to refraction and double structure artifacts in conventional image compounding. These effects may be avoided if a correction process is carried out for each partial image before composition. Ray tracing algorithms can be used to allocate refracted samples of A-Scans based on a speed of sound map obtained with transmission tomography. However, correction may be also achieved extracting information directly from partial images (Bartelt, 1988). In this work, the imaged object was assumed to be homogeneous, although with a speed of sound different from that of the coupling medium (water), namely c_1 . To obtain a speed of sound map, since the A-Scans acquired from opposite directions insonify the same scatterers, the maximum of their cross correlation provides an estimation of the speed of sound in the imaged object.

Let $r_l(t)$ and $r_r(t)$ two A-Scans acquired from opposed angular positions, and T_{TNK} the time of flight between them in water. The correlation between $r_l(t)$ and the inverted version $r_r(T_{TNK} - t)$ peaks at Δt , which is the difference of times of flight (TOF_l and TOF_r) to a virtual scatterer observed from two opposed directions.

$$\Delta t = (TOF_l + TOF_r) - T_{TNK} \quad (5)$$

When the times of flight are decomposed depending on the propagation media, the speed of sound of the imaged object c_2 is obtained.

$$c_2 = \left(\frac{\Delta t}{2W_{ph}} + \frac{1}{c_1} \right)^{-1} \quad (6)$$

where W_{ph} is the imaged object width, obtained after estimating the interface between the two media. For each angular position of the array probe, the interface is detected by applying a threshold to the A-Scan at 0° steering angle after a moving average filtering. A smooth and closed curve is interpolated with the collected samples. The refraction of incident rays (A-Scans) is computed applying the Snell law. Then, each sample is allocated according to the corresponding time-of-flight and speed of sound.

2.3. Transmission tomography

2.3.1. Time-of-flight sinograms

In ultrasound tomography, the time-of-flight (TOF) is known as the elapsed time since the signal emerges from the emitter transducer until the first reflected signal arrives to the receiver transducer. It can be calculated as follows:

$$TOF = \int \frac{1}{c^2} dl = \int s^2 dl \quad (7)$$

where c is the sound speed, s is the slowness and l is the path length of the wave front.

If straight trajectories are assumed, once the object is scanned from different angles covering projections between 0 - 360° and TOF values are recorded for all emitter-receiver pairs, we will have a suitable data set to be reconstructed by using inverse radon transform. For this purpose, we stored the entire data into sinograms (Fahei, 2002).

2.3.2. FBP and 2D OSEM methods

The FBP algorithm (Herman, 1980) is a commonly used technique in medical image reconstruction (CT, PET and SPECT). In FBP, the Fourier transform of each projection is multiplied by a ramp filter in the frequency domain. Then, the inverse Fourier transform is applied and the resulting data are back-projected to form the image. It is a very fast technique but it has major disadvantages like poor resolution and low signal to noise ratio. This process can be easily implemented in MATLAB once the data are stored in form of sinograms.

Iterative solutions for image reconstruction are often considered much better quality. Calculations are repeated, and hence, the following iteration is always slightly better than the previous one. The iteration continues until errors reach a prescribed limit. In this sense, the Order Subset Expectation Maximization algorithm (Hudson and Larkin, 1994) is one of the most used methods when working with rectilinear trajectories, basically because of its fast performance and high quality results. This algorithm is based in ML-EM (Shepp and Vardin, 1982). Here the projection data are grouped into ordered subsets, where each subset contains a set of regularly spaced projections. The subset number is the speed-up factor and the sum of counts in projections forming the subsets is equal for all subsets. It is also very easy to implement in Matlab by means of the straight forward and inverse Radon transform.

2.3.3. Experimental setup and phantom description

All the experimental measurements in tomographic mode were performed with the same system described in section 2.1. In this case, 23 fan-beams were employed with step angles of 15 degrees between them. A total of 128 elements per fan-beam were employed to emit and receive, and each emitter element was made to correspond with 10 receiver elements. The total measurement time for this initial prototype was 3 hours.

We also developed an agar-glycerine-gelatine phantom to test our system. Its major characteristics can be seen in Figure 2 and Table 1. Three holes were formed inside the phantom and filled with water.



Fig 2. (a) Front view of the phantom, (b) top view and (c) scheme of the top view

Table 1. Composition and size of the phantom

Water (ml)	Glycerin (ml)	Gelatine (g)	Agar (g)	Height (mm)	External diameter (mm)	Expected sound speed (m/s)
720	180	50	20	98	102	1560

3. Results

3.1. FASC images

Figure 3a shows a conventional sector image, taken when the array probe is at $\varphi = 180^\circ$. Image quality deteriorates at the rightmost part of the image due to worse resolution with depth and to refraction effects. Figure 3b shows the FASC of 36 conventional reflection images, taken at regular-angle positions. As all insonification angles are covered, biological structures are fully depicted and spatial resolution is homogeneous. Moreover, speckle variance is reduced by the spatial compounding. Figure 3c shows the result when refraction is corrected. This yielded a correction of double structures and shape distortions. Some relevant biological structures are depicted in Fig. 4, for which Contrast Ratio (CR) and Noise to Contrast Ratio (CNR) were evaluated. CNR improves with compounding (e.g. 14 dB to 19 dB in the hyperechoic cyst, fig. 4a), while CR remains practically unchanged.

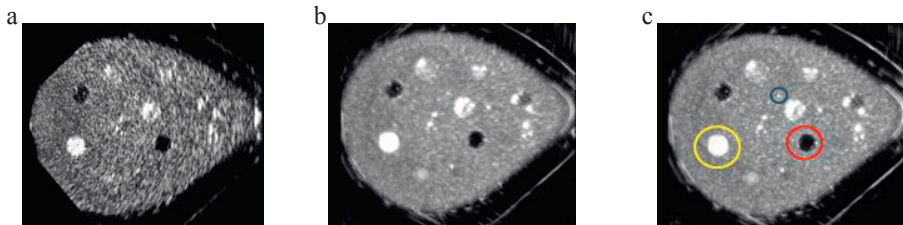


Fig 3. (a) Sectorial B-Mode image acquired at 180° ; (b) Spatial compounding of 36 sectorial images without refraction correction; (c) FASC of 36 sectorial images after refraction correction

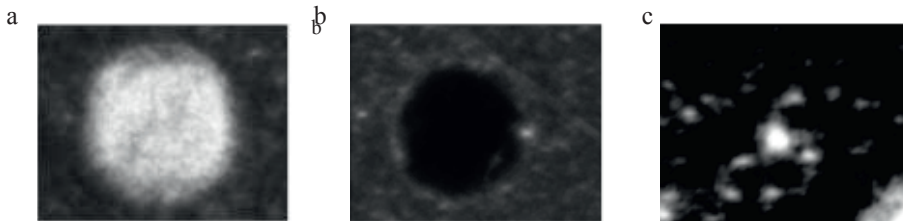


Fig 4 (a) Hiperechoic cyst detail (yellow circle in Fig5c); (b) Anechoic cyst detail (red); (c) Microcalcification detail (blue)

3.2. Tomographic images.

The TOF data was arranged into a 2-D sinogram with 600 radial bins and 600 angular bins. With this configuration, the expected maximum resolution achievable is 0.33 mm, which is worse than $\lambda/2$ expected due to the use of ray tracing algorithms. Nevertheless, it is good enough to see major lesions presented in the phantom except the needle with 0.2 mm of diameter. The sinogram and reconstructed images can be seen in Fig. 5 a, b and c respectively.

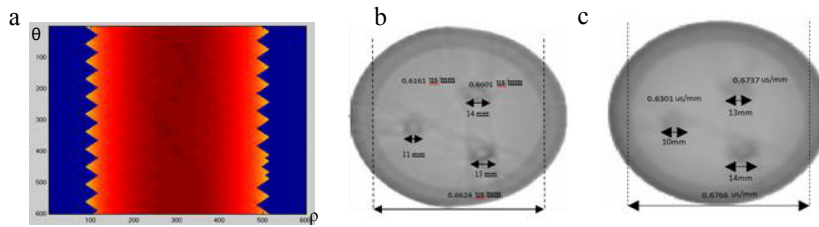


Fig 5. (a) Sinogram of the acquired data (b) reconstructed image with FBP algorithm (c) reconstruction image with OSEM algorithm.

These images were reconstructed in 0.3 and 30 seconds for FBP and OSEM respectively, using one single core of an 8 core, 2.2 GHz CPU. For both cases, adequate values of slowness and a correct location of lesions were achieved. It can be noticed the better image quality obtained with the OSEM algorithm, as the FBP image shows some artefacts at the edges of the cylindrical holes. This demonstrates that even when a less than realistic model is employed (i.e. ray-tracing), the iterative method is capable of recovering most of the information present in these data.

4. Conclusions

An improved parametric spectral procedure applied in laboratory, to estimate shifts in PSD of ultrasonic echoes from an arterial phantom with a 10-MHz transducer, shows promising responses for a non-invasive measurement of small thicknesses alterations in the walls of arterial phantoms. Good spatial resolutions can be potentially attained: of an order of micron, which are clearly better than those attained in walls with non-parametric spectral techniques or using conventional time cross-correlation. The reason is that our parametric spectral procedure presents frequency lobes narrower than other spectral options, in the overtones of the resonant echoes returning from an arterial wall.

For instance, by using the 10th overtone of the resonant wall echo, a reasonable frequency definition of 19.5 kHz is obtained, which represents a excellent spatial resolution of ($\pm 0.9 \mu\text{m}$), clearly improving the spatial performance of the methods based on the periodogram or on cross-correlation operators, which provide resolutions around 20-30 μm , $\pm 11 \mu\text{m}$ in the best scenario of signal to noise ratio.

New experimental efforts and additional analyses with complex ultrasonic echoes, acquired from well-controlled sanguineous tissues patterns, are still needed, to select the best spectral algorithm for distinct cases and optimize the potential resolution of this recent approach. In addition, possible clinical limitations must be evaluated.

Acknowledgements

Luis Medina wishes to acknowledge the Spanish Ministry of Economy and Competitiveness for the financial support (grant BES-2011-048124).

References

- Bartelt H. Computation of local directivity, speed of sound and attenuation from ultrasonic reflection tomography data. *Ultrasonic Imaging* 1988; 10:110-120
- Breast cancer. (2014). Retrieved May 20, 2014, from <http://www.cancer.org/cancer/breastcancer>.
- Fahei F. Data Acquisition in PET Imaging. *Journal Of Nuclear Medicine Technology* 2002; 30(2):39-49
- Herman G. Image reconstruction from projections: the fundamentals of computerized tomography, Academic Press 1980.
- Hudson H. and Larkin R. Accelerated image reconstruction using ordered subsets of projection data. *Medical Imaging, IEEE Transactions on*, 1994;13, 601-609.
- Jemal A, Bray F, Center MM, Ferlay J, Ward E, Forman D. Global cancer statistics. *CA Cancer J Clin* 2011; 61:69-90.
- Ranger B, Littrup PJ, Duric N, Chandiwalla-Mody P, Li C. Schmidt S, Lupinacci J. Breast ultrasound tomography versus magnetic resonance imaging for clinical display of anatomy and tumor rendering: Preliminary results. *AJR Am J Roentgenol* 2012; 198(1):233-239

- Roy O, Schmidt S, Li C, Allada V, West E, Kunz D, Duric N. Breast imaging using ultrasound tomography: From clinical requirements to system design. *Joint UFFC, EFTF and PFM Symposium* 2013; 1174-1177.
- Schomberg H. An improved approach to reconstructive ultrasound tomography. *J. Phys. D: Appl. Phys.* 1978; 11:L181-L186.
- Shepp L and Vardi Y. Maximum Likelihood Reconstruction for Emission Tomography. *Medical Imaging, IEEE Transactions on*, 1982; 1, 113-122
- Ursin G, Hovanesian-Larsen L, Parisky YR, Pike MC, Wu AH. Greatly increased occurrence of breast cancers in areas of mammographically dense tissue. *Breast Cancer Research* 2005; 7:R605-R608
- Wiskin J, Borup D, Johnson S, Berggren M, Robinson D, Smith J, Chen J, Parisky Y, Klock J. Inverse scattering and refraction corrected reflection for breast cancer imaging. *Proc. SPIE Medical Imaging* 2010; 7629:76290K